ChemComm

Accepted Manuscript

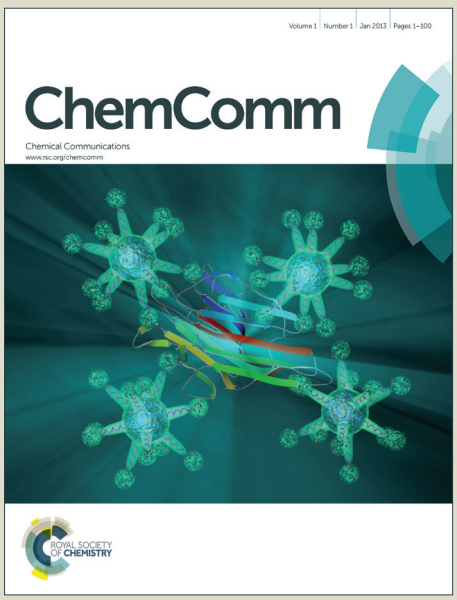

ROYAL SOCIETY OF CHEMISTRY

www.rsc.org/chemcomm

Table of Contents:

Selective Hg^{2+}-binding of click-derived triazole-based amphiphiles can lead to the formation of nanostructures, even below CMCs, which are determined by the stoichiometry of amphiphile-Hg^{2+}complexes affecting the interfacial curvature.

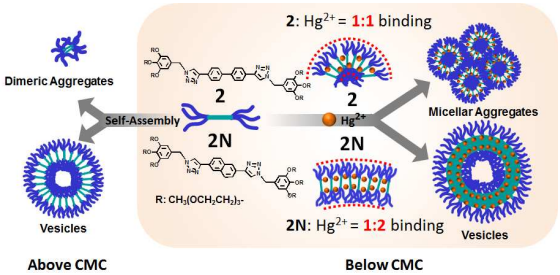

ChemComm RSCPublishing

COMMUNICATION

Micellar and vesicular nanoassemblies of triazole-based amphiphilic probes triggered by mercury(II) ions in a 100% aqueous medium

Cite this: DOI: 10.1039/x0xx00000x

Received 00th January 2014,
Accepted 00th January 2014

DOI: 10.1039/x0xx00000x

www.rsc.org/chemcomm

Inhye Kim,[a] Na-Eun Lee,[a] Yoo-Jeong Jeong, [a] Young-Ho Chung,[b] Byoung-Ki Cho,*[c] and Eunji Lee*[a,b]

ABA-type amphiphiles bearing a triazole-based aromatic block were easily synthesized using click chemistry, which act as a fluorescent turn-off Hg^{2+}-chemoprobe in an aqueous solution. Interestingly, the metal-binding process of amphiphiles induced nanoassemblies even below the CMCs, and the binding stoichiometry affected the morphologies of the resultant nanostructures.

Stimuli-responsive nanomaterials alter their physical properties according to a small change of environment. These systems have gained increasing attention in a variety of applications such as catalysis, sensors, drug delivery, tissue engineering, and diagnostics, etc.[1] Among the molecular scaffolds, the fluorophore-conjugated molecules, in response to specific metal ions, have contributed to the development of chemosensors possessing fluorescence "on-off" signals which are attributed to the charge transfer, photo-induced energy transfer (PET) process and excimer formation.[2] However, most of them have been designed on the basis of small organic fluorophores, and the signaling events have occurred at a single molecular level. Furthermore, they could not form nanoaggregates in an aqueous solution due to low solubility,[3] so it is hard to achieve easy processability of aqueous metal ion sensors for a variety of nanomaterial-based applications. In this context, aromatic amphiphiles containing an active block for metal ion binding can be considered as aqueous fluorescence nanoprobes that can overcome the limits of single molecular systems.[4] This is because amphiphiles based on the emissive aromatic unit and flexible coil can self-assemble into various core/shell nanostructures, including spheres, cylinders and vesicles.[5]

"Click chemistry" has received much interest in green-chemistry and biomedicals[6] due to its biocompatibility, synthetic simplicity, and mild reaction conditions, which results in fluorescent 1,4-disubstituted 1,2,3-triazole derivatives.[7] This click-derived triazole moiety has been known to play a role as a ligand offering several donor sites for metal coordination[8] as well as a part of conjugated fluorophore providing a significant number of chemosensors.[9] Therefore, one can envision that the design of emissive amphiphiles mediated by click chemistry would provide a facile route for the fabrication of aqueous nanostructured probes in response to metal ions.

Meanwhile, the development of fluorescent chemosensors for selective detection of Hg^{2+} in the human body and the environment is of paramount importance because Hg^{2+} is toxic and hazardous to several species, causing disorders and damage to brain, central nervous system, endocrine system and kidney[10] as well as a bioaccumulation in the human body.[11] However, the design of aqueous probes is still challenging due to the strong hydration ability of Hg^{2+} in an aqueous medium.[12]

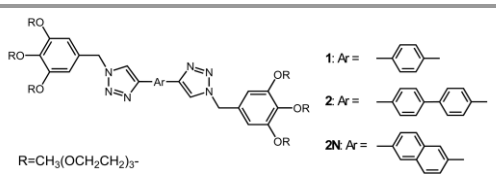

Scheme 1 Molecular structure of ABA-type amphiphilic molecules **1**, **2**, and **2N**; aromatic moiety is denoted by **Ar**.

To this end, we designed ABA-type amphiphilic molecules based on triazole-based aromatic segments and hydrophilic tri(ethylene oxide) peripheries (Scheme 1), and investigated their assembly behaviour and optical response on various metal ions in 100% aqueous solution. The subtle change in the aromatic segment caused significantly different aggregation (Fig. 1). In particular, the higher binding affinity of amphiphiles to Hg^{2+} was observed, and it reinforced the formation of well-defined nanoaggregates (even below their critical micellar concentrations (CMC)) accompanied by a fluorescence "turn-off". In this paper, the mechanistic aspect for the morphologies of selectively Hg^{2+}-captured amphiphiles is highlighted.

The aromatic amphiphiles **1**, **2**, and **2N** were prepared by Cu(I)-catalyzed cycloaddition (click reaction) of azide-terminated benzyl ether dendron and diethynyl precursors.[13] In an aqueous solution (20

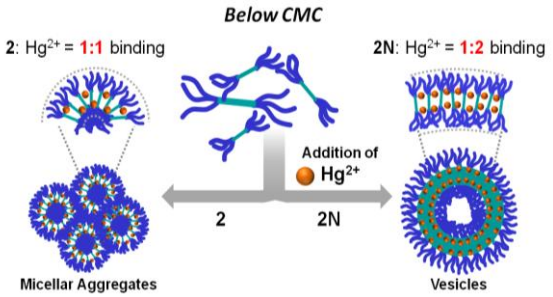

Fig. 1 Schematic representation of Hg^{2+}-induced nanostructure of **2** and **2N;** CMC is defined as the concentration of amphiphiles above which aggregates form.

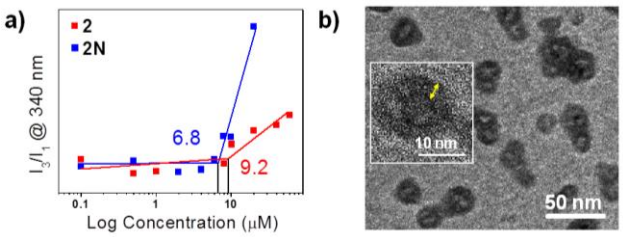

Fig. 2 (a) Determination of the CMCs of **2** and **2N**. (b) TEM image showing the presence of vesicular structures of **2N** (yellow arrow in the inset image, wall thickness).

μM), the emission spectra of all molecules were shown to be different from each other. Molecule **1** with the shortest aromatic block showed a weak emission (Fig. S2b). It displayed only a slight quenching of fluorescence at 327 nm (λ_{ex}= 276 nm) by replacement of chloroform with water. Amphiphile **2** based on the biphenyl moiety exhibited an obvious quenching of emission in the aqueous solution, as compared to the chloroform solution (Fig. S2b). This is due to the energy transfer between the aromatic segments, which indicates the aggregation of amphiphiles.[14] In contrast, the emission of **2N** containing a naphthalene moiety was enhanced, even though it has a similar conjugated aromatic length to **2** (Fig. S2d). This emission enhancement of **2N** may be attributed to the conformational restriction by the fused ring structure of the naphthalene, which is known as the aggregation induced emission enhancement (AIEE).[15]

The CMC was determined by a fluorescence spectrometer using pyrene as a hydrophobic substance (Fig. 2a).[16] Amphiphile **1** did not show the CMC. In contrast, the CMCs of **2** and **2N** were calculated to be approximately 9.2 μM and 6.8 μM, respectively. Interestingly, above the CMC (20 μM), the transmission electron microscopy (TEM) image of **2** did not show any noticeable aggregates, while that of **2N** displayed well-defined vesicular nanostructures with a wall thickness of about 5 nm (Fig. 2b), which could be identified by the contrast between the peripheral and central areas of the aggregates (Fig. 2b, inset).[17] Considering the extended molecular length of **2N** (*ca.* 4.8 nm, Fig. S3a), the evaluated wall thickness of ~5 nm indicates that the vesicle membrane consists of a monolayer packing arrangement of **2N**. The distinct aggregation ability between the amphiphiles can be explained by hydrophilic/hydrophobic balance between the oligoether dendron and hydrophobic aromatic blocks.[18] The aromatic block of **1** may be too short to form aggregates so that the increase in the number of aromatic rings (**2** and **2N**) induced the self-organization of amphiphiles through enhanced π-stacking. Molecules **2** and **2N** formed the aggregates to avoid unfavorable contacts between the hydrophobic block and water. However, **2** still has a tenuous assembly capability, resulting in the dimeric aggregates as shown in the DLS data (Fig. S4). Only **2N** with enhanced coplanarity of the aromatic blocks could assemble into well-defined nanostructures.

The metal-binding ability of the amphiphiles was examined using the various metal ions, including $Hg(ClO_4)_2$, $CuSO_4$, $ZnSO_4$, $CaCl_2{\cdot}2H_2O$, $Pb(NO_3)_2$, $Al(NO_3)_3{\cdot}9H_2O$, and $MgSO_4$ (Figs. 3a,b and S5). Since molecule **1** did not form any aggregates, the binding selectivity of all molecules toward metal ions was investigated at a concentration below CMC (5 μM) for fair comparison. Overall, the emission of amphiphiles progressively decreased with an increase in the amount of metal ions, which indicates a coordination of metal ion with the triazole units.[19] However, **1** did not show any noticeable binding affinity (Fig. S5). In particular, **2** exhibited a good selectivity to Hg^{2+} (Fig. 3a). The suppression in the emission was observed upon the addition of Hg^{2+} to the aqueous solution of **2** (*ca.* 2/5 (a. u.) quenching upon the addition of 100 equiv. of Hg^{2+}). This is due to a heavy metal ion effect or a reverse PET (Fig. S6a).[20] Interestingly, **2N** showed a high affinity to Hg^{2+} as well as Cu^{2+}.[21] The strong quenching of the emission appeared even upon addition of 1 equiv. of Hg^{2+} and Cu^{2+}, respectively, (*ca.* 4/5 and 9/10 (a. u.) quenching, Figs. S6b,c). By comparing the degrees of fluorescence quenching of **2** and **2N** upon addition of the equal equivalent Hg^{2+} (Fig. S6), it was concluded that the **2N** has a higher binding affinity to Hg^{2+} metal ions than **2**. In detail, the association constants (K_a) of **2** and **2N** for Hg^{2+} were evaluated to be 1.24×10^4 M^{-1} and 3.06×10^5 M^{-2} by a non-linear fitting curve method, respectively (Fig. S8),[22,24] indicating that the interaction of **2N** with Hg^{2+} is stronger than **2**.

Remarkably, after forming amphiphile-Hg^{2+} complex, the TEM images of both **2** and **2N** showed the formation of nanoaggregates even though the concentrations of the aqueous solution were below their CMCs. The **2**-Hg^{2+} and **2N**-Hg^{2+} complexes formed spherical aggregates with diameters of 10-20 nm and 60-90 nm, respectively (Figs. 3c,d). In the conventional TEM image of **2**-Hg^{2+}, no significant contrast was revealed in the spherical aggregate, which suggests that the aggregate is not a vesicle. Instead, the large spheres of **2**-Hg^{2+} seem to be composed of elemental spherical micelles.[23] On the other hand, the aggregates of **2N**-Hg^{2+} displayed the deflated nature resulting from the evaporation of water (Fig. 3d). The cryogenic-TEM (cryo-TEM) image of the solution of **2N**-Hg^{2+} in the inset of Fig. 3d clearly showed that the inner cavity of the spheres is full of water, thus confirming the vesicular structure.

To elucidate the different molecular assemblies between **2**-Hg^{2+} and **2N**-Hg^{2+}, we first investigated the binding stoichiometries by Job's plot method. The stoichiometric ratios of **2**:Hg^{2+} and **2N**:Hg^{2+} were determined to be 1:1 and 1:2, respectively (Figs. 4a,b). Next, to understand such Hg^{2+}-binding modes in the molecular level, ^{1}H-NMR experiments were carried out and the chemical shift changes were examined. Upon addition of 1.0 equiv. of Hg^{2+} to the solution of **2**, the triazolyl H_c and benzylic H_b were shifted downfield by 0.14 ppm and 0.06 ppm, respectively (Fig. 4c). These changes imply that Hg^{2+} was bound to a triazolyl nitrogen.[23] Similarly, the triazolyl H_c and benzylic H_b of **2N** were shifted downfield by 0.18 ppm and 0.10 ppm,

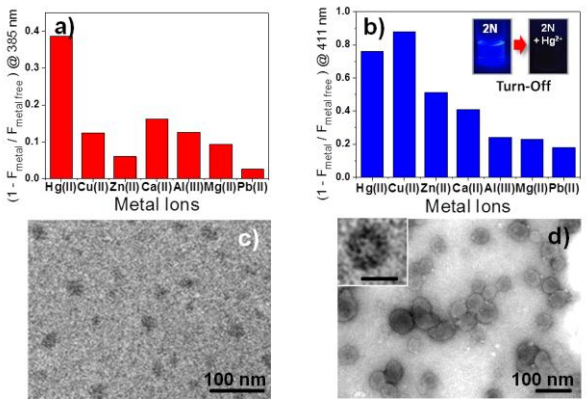

Fig. 3 (a,b) The binding selectivity of **2** and **2N** toward Hg^{2+} and other metal ions. The fluorescence measurements were performed in aqueous solutions and in the absence and presence of 4.0 equiv. of a metal ion (inset of (b), fluorescence photographs of a solution of sensors (5 μM) excited by a commercially available UV lamp (λ_{ex} = 365 nm)). TEM images of (c) **2**-Hg^{2+} and (d) **2N**-Hg^{2+}, respectively (c), non-stained image; (d) negatively-stained image; inset of (d), cryo-TEM image of vesicular structures of **2N**-Hg^{2+}, scale bar= 10 nm.

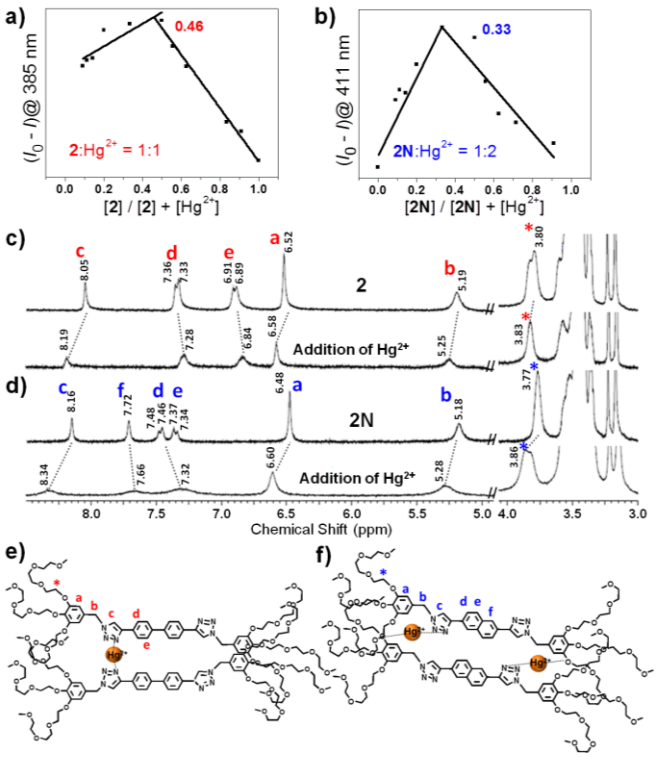

Fig. 4 Fluorescence Job's plot for determination of stoichiometries of (a) **2**-Hg^{2+} and (b) **2N**-Hg^{2+}, respectively. ^{1}H NMR (300 MHz) spectra of (c) **2** and (d) **2N** (5mM) in the absence (top) and presence (bottom) of 1 equiv. of Hg^{2+} in D_2O. Possible Hg^{2+}-binding modes of (e) **2** and (f) **2N**.

respectively (Fig. 4d). It is worth noting that the extent of the chemical shift changes is in agreement with the association constants calculated from the emission spectra results suggesting the stronger affinity of **2N** toward Hg^{2+} than **2** (Fig. S8). Interestingly, in contrast to the small change (by 0.03 ppm) of the H* in the NMR spectra of **2**, the H* of **2N** showed a significant downfield shift of 0.09 ppm upon addition of Hg^{2+}. This result means that Hg^{2+} in **2N**-Hg^{2+} complex also had a strong interaction with the oxygen atoms next to the phenyl group.[23] Thus, we supposed that this binding mode may be attributed to a strong tendency of **2N** with enhanced π-π interaction to maintain the tight packing of aromatic blocks. On the basis of these results, the plausible binding models of **2**-Hg^{2+} and **2N**-Hg^{2+} were proposed in Figs. 4e and f, respectively. As a result, the morphological differences between the **2**-Hg^{2+} and **2N**-Hg^{2+} are possibly explained in terms of the Hg^{2+}-binding mode in aqueous solution. The **2**-Hg^{2+} complex showing 1:1 stoichiometry of **2** to Hg^{2+} may pack loosely which leads to a micellar structure with high interfacial curvature.[24] On the other hand, the 1:2 stoichiometry of the **2N**-Hg^{2+} complex enforces the tight packing, which favours a better-organized flat interface between the hydrophobic core and hydrophilic corona. Consequently, **2N**-Hg^{2+} formed the vesicles.

In addition, direct evidence for the triazole-based amphiphile-Hg^{2+} complexes could be obtained by Fourier transform infrared spectroscopy (FTIR) experiments.[25] After the addition of Hg^{2+} to the aqueous solution of **2** and **2N**, the Hg-N stretching vibration band appeared at 587 cm^{-1} (Fig. S9a), indicating the coordination of triazolyl nitrogen to the metal atom. Furthermore, the high angle annular dark-field scanning TEM (HAADF-STEM) measurements were carried out to confirm the existence of Hg^{2+} within the hybrid vesicles (Fig. S9b). The image showed a clear contrast, exhibiting the presence of organic-inorganic hybrid vesicular structures against to the black background (Fig. S9b, top left). Energy dispersive X-ray spectroscopy (EDS) elemental maps could prove that Hg^{2+} ions were concentrated in the vesicles (Fig. S9b, top right). Therefore, we concluded that the Hg^{2+} can join the neighboring amphiphiles by interacting with the triazolyl moieties which induces the molecular assembly to form the nanostructures with enhanced stability, in addition to the inherent ability of the amphiphiles to form the aggregates in aqueous solution.

Considering the growing applications of click chemistry in material science,[13] the nanostructure formation of triazole-based amphiphile-Hg^{2+} conjugates in this study would provide a useful and simple strategy for the fabrication of nano-chemosensor for detection of toxic heavy metals in water. In addition, the resultant vesicular hybrids induced by the response to particular metal ion would open up the development of stimuli-responsive functional nanovehicles.

This research was supported by Basic Science Research Program (2013R1A1A2061197) through the National Research Foundation of Korea (NRF) funded by the Korea Government (MEST), Korea Basic Science Institute grant (D34402), and Chungnam National University Research Fund.

Notes and references

[a]*Graduate School of Analytical Science and Technology, Chungnam National University, Daejeon 305-764, Republic of Korea. Fax: 82 42 821 8541; Tel: 82 42 821 8548; E-mail: eunjilee@cnu.ac.kr*
[b]*Division of Life Science, Korea Basic Science Institute, Daejeon 305-806, Republic of Korea.*
[c]*Department of Chemisty, Dankook University, Gyeonggi-Do 448-701, Republic of Korea. E-mail: chobk@dankook.ac.kr*

†Electronic Supplemenraty Information (ESI) available: Detailed synthetic and experimental procedures. See DOI: 10.1039/b000000x/

1. M. A. C. Stuart, W. T. S. Huck, J. Genzer, M. Müller, C. Ober, M. Stamm, G. B. Sukhorukov, I. Szleifer, V. V. Tsukruk, M. Urban, F. Winnik, S. Zauscher, I. Luzinov and S. Minko, *Nat. Mater.*, 2010, **9**, 101-113.
2. L. Prodi, F. Bolletta, M. Montalti and N. Zaccheroni, *Coord. Chem. Rev.*, 2000, **205**, 59-83.
3. H. N. Kim, W. X. Ren, J. S. Kim and J. Yoon, *Chem. Soc. Rev.*, 2012, **41**, 3210-3244.
4. I. Kim, H.-H. Jeong, Y.-J. Kim, N.-E. Lee, K.-m. Huh, C.-S. Lee, G. H. Kim and E. Lee, *J. Mater. Chem. B*, 2014, **2**, 6478-6486.
5. J. Zhang, X.-F. Chen, H.-B. Wei and X.-H. Wan, *Chem. Soc. Rev.*, 2013, **42**, 9127-9154.
6. (*a*) S. K. Mamidyala and M. G. Finn, *Chem. Soc. Rev.*, 2010, **39**, 1252-1261; (*b*) N. J. Agard, J. A. Prescher and C. R. Bertozzi, *J. Am. Chem. Soc.*, 2004, **126**, 15046-15047.
7. H. C. Kolb, M. G. Finn and K. B. Sharpless, *Angew. Chem. Int. Ed.*, 2001, **40**, 2004-2021.
8. H. Struthers, T. L. Mindt and R. Schibli, *Dalton Trans.*, 2010, **39**, 675-696.
9. Y. H. Lau, P. J. Rutledge, M. Watkinson and M. H. Todd, *Chem. Soc. Rev.*, 2011, **40**, 2848-2866.
10. P. B. Tchounwou, W. K. Ayensu, N. Ninashvili and D. Sutton, *Environ. Toxicol*, 2003, **18**, 149-175.
11. F. M. M. Morel, A. M. L. Kraepiel, M. Amyot, *Annu. Rev. Ecol. Syst.*, 1998, **29**, 543-566.
12. (*a*) Y. Wu, Y. Dong, J. Li, X. Huang, Y. Cheng and C. Zhu, *Chem. Asian J.*, 2011, **6**, 2725-2729; (*b*) A. Ono and H. Tohashi, *Angew. Chem. Int. Ed.*, 2004, **43**, 4300-4302; (*c*) W. Huang, X. Zhu, D. Wua, C. He, X. Hu and C. Duan, *Dalton Trans.*, 2009, 10457-10465; (*d*) M.-H. Yang, P. Thirupathi and K.-H. Lee, *Org. Lett.*, 2011, **13**, 5028-5031.
13. V. V. Rostovtsev, L. G. Green, V. V. Fokin and K. B. Sharpless, *Angew. Chem.*, 2002, **114**, 2708-2711.
14. B. W. Messmore, J. F. Hulvat, E. D. Sone and S. I. Stupp, *J. Am. Chem. Soc.*, 2004, **126**, 14452-14458.
15. Q. Zeng, Z. Li, Y. Dong, C. Di, A. Qin, Y. Hong, L. Ji, Z. Zhu, C. K. W. Jim, G. Yu, Q. Li, Z. Li, Y. Liu, J. Qin and B. Z. Tang, *Chem. Commun.*, 2007, 70-72.
16. K. Kalyanasundaram and J. K. Thomas, *J. Am. Chem. Soc.*, 1977, **99**, 2039-2044.
17. M. Yang, W. Wang, F. Yuan, X. Zhang, J. Li, F. Liang, B. He, B. Minch and G. Wegner, *J. Am. Chem. Soc.*, 2005, **127**, 15107-15111.
18. E. Lee, Y.-H. Jeong, J.-K. Kim and M. Lee, *Macromolecules*, 2007, **40**, 8355-8360.
19. A. P. de Silva, H. Q. N. Gunaratne, T. Gunnlaugsson, A. J. M. Huxley, C. P. McCoy, J. T. Rademacher and T. E. Rice, *Chem. Rev.*, 1997, **97**, 1515-1566.
20. (*a*) M. Choi, M. Kim, K. D. Lee, K.-N. Han, I.-A Yoon, H.-J. Chung and J. Yoon, *Org. Lett.*, 2001, **3**, 3455-3457; (*b*) M.-Y. Chae, X. M. Cherian and A. W. Czarnik, *J. Org. Chem.*, 1993, **58**, 5797-5801.
21. The molecule **2N** can bind the Cu^{2+}, which results in the formation of vesicles. See Figs. S6c,d, S10 and S11 in SI.
22. P. Thordarson, *Chem. Soc. Rev.*, 2011, **40**, 1305-1323.
23. X. Liu, X. Yang, Y. Fu, C. Zhu and Y. Cheng, *Tetrahedron*, 2011, **67**, 3181-3186.
24. Y. Mai and A. Eisenberg, *Chem. Soc. Rev.*, 2012, **41**, 5969-5985.
25. M. Hanif and Z. H. Chohan, *Spectrochim. Acta A Mol. Biomol. Spectrosc.*, 2013, **104**, 468-476.